

Assessment of the World Wide Lightning Location Network (WWLLN) detection efficiency by comparison to the Lightning Imaging Sensor (LIS)

Running head: WWLLN detection efficiency relative to LIS

Rodrigo E. Bürgesser

Group of Atmospheric Physics, FaMAF, Universidad Nacional de Córdoba, IFEG-
CONICET, Córdoba, Argentina.

Corresponding author: Rodrigo Bürgesser, burgesse@famaf.unc.edu.ar. FAMAFA,
Ciudad Universitaria, 5000 Córdoba, Argentina.

Abstract

In this study, strokes detected by the World Wide Lightning Location Network (WWLLN) were compared to the flashes detected by the Lightning Imaging Sensor (LIS) between the years 2012 and 2014. To evaluate the WWLLN detection efficiency, the strokes detected by WWLLN in the field of view of LIS were determined and matched with the flashes detected by LIS. The spatial and time distribution of the strokes detected by WWLLN show a good correlation with the flashes detected by LIS despite the low detection efficiency reported for WWLLN. The analysis shows that WWLLN is capable of detecting more than one stroke per flash with a global multiplicity of 1.5. However, not all strokes detected by WWLLN in the field of view of LIS could be assigned to a flash. These unmatched strokes show a spatial and time distribution, as well as an energy distribution, similar to those of the matched strokes. The unmatched strokes seem to correspond to cloud-to-ground flashes which are not well detected by LIS. Based on matched flashes and multiplicity, a correction of the WWLLN data was derived. With this correction, a global lightning flash rate of 60 fl s^{-1}

This article has been accepted for publication and undergone full peer review but has not been through the copyediting, typesetting, pagination and proofreading process, which may lead to differences between this version and the Version of Record. Please cite this article as doi: 10.1002/qj.3129

was obtained and a map of the corrected flash density detected by WWLLN was performed. The spatial distribution of WWLLN multiplicity and detection probability are available for the community.

Keywords: Lightning; Detection efficiency; WWLLN; LIS.

Introduction

Lightning data are widely used in many different fields. For instance, lightning data are used for aviation operations, insurance companies and meteorological agencies. Many studies have been using lightning data as a proxy to detect thunderstorms (Mecikalski et al., 2013; Xu et al., 2013), to generate alerts for severe weather (Schultz et al., 2011; DeMaria et al., 2012), and as an indicator of climate change (Reeve and Toumi, 1999; Romps et al., 2014). The discharge process and the different atmospheric processes, where lightning has a fundamental role, are research topics in which much effort has been invested in the past years. Thus, the importance of lightning data has led to the development of several detection systems with the purpose of obtaining high quality data.

The Lightning Imaging Sensor (LIS), on board the Tropical Rainfall Measuring Mission satellite (TRMM, <http://thunder.msfc.nasa.gov>) has been operated from December 1997 to April 2015, providing lightning data over the tropical region of Earth (Christian et al., 1992; Boccippio et al., 2002). However, due to the satellite movement, the observation time of a given location is about 80s (Christian et al., 2000) and, therefore, LIS provides high quality lightning data for discrete times. This data is good enough to generate lightning annual climatology but not to study the time evolution of a given storm or a storm system.

With the launch of the Geostationary Operational Environmental Satellite R series (GOES-R) (now GOES-16), a new optical sensor, the Geostationary Lightning Mapper, was deployed to continuously detect the lightning activity over America and its adjacent ocean region. The Geostationary Lightning Mapper (GLM) is an optical sensor that detects total lightning (in-cloud, cloud-to-cloud and cloud-to-ground) activity over the western hemisphere (<http://www.goes-r.gov/>). The GLM delivers lightning measurements similar to those of LIS but it provides a continuous lightning detection. Therefore, this instrument will provide high quality data for forecasting severe storms and convective weather but only over America and its adjacent ocean region (Goodman et al., 2013).

Different ground-base lightning detection networks, regional and global, have been developed to provide real and continuous detection over time. Short range lightning detection network such as the Lightning Detection Network (LINET, Betz et al., 2009), the National Lightning Detection Network (Cummins and Mur, 2009), and the Canadian Lightning Detection Network (Dockendorff and Spring, 2005) provide regional coverage of total lightning with high detection efficiency but these networks do not provide information over oceanic regions or remote locations. The development of long range detection networks such as the World Wide Lightning Location Network (WWLLN, <http://wwlln.net>), Vaisala GLD360 (Vaisala, 2009) and the Earth Networks Total Lightning Network (ENTLN; Heckman, 2014) allow a world-wide and real time lightning detection but with a lower detection efficiency than short range detection networks and satellite detection systems.

The World Wide Lightning Location Network (WWLLN, <http://wwlln.net>) was developed as an answer to the need of a world-wide and real time detection system. This network can provide quality lightning data over oceanic and remote regions, where

regional networks are not operational. The network also presents a continuous detection over time which is not provided by satellite instruments. The lightning data provided by WWLLN has been used in many studies (e.g. Soula et al., 2016; Shevtsov et al., 2015; Virts et al., 2015; Garreaud et al., 2014), but a better characterization of WWLLN detection efficiency would be beneficial and would allow a more extensive use of the lightning data provided by this network. Several attempts have been made to study the detection efficiency and the location and time accuracy of WWLLN (Abarca et al., 2010; Abreu et al., 2010; Hutchins et al., 2012a; Rudlosky and Shea, 2013; Thompson et al., 2014; among others).

Abarca et al. (2010) used the lightning data provided by the National Lightning Detection Network (NLDN) to assess the WWLLN capability over the United States between 2006 and 2009. These researchers found an improvement on the WWLLN capability to detect cloud-to-ground flashes over the years, with a bias of the network to detect the most energetic flashes. Abreu et al. (2010) evaluated the WWLLN data during 2008 using the lightning data of the Canadian Lightning Detection Network (CLDN). The study was performed on the lightning data detected over a region centered on southern Ontario (Canada) and found that WWLLN is most sensitive to high peak current lightning strokes. Also, this study showed that changes in the ionosphere affect the WWLLN detection efficiency with a better ability of the network during local midnight and worst ability during local noon. Rudlosky and Shea (2013) evaluated the lightning data provided by WWLLN relative to the data provided by LIS during 2009-2012 over the western hemisphere. In this study, flashes detected by LIS were matched with strokes detected by WWLLN to determine the detection efficiency of WWLLN relative to LIS. They found an improvement in the detection efficiency of WWLLN through the analyzed years over the region under study. Thompson et al. (2014)

compared the lightning group's data detected by LIS with the lightning stroke data detected by WWLLN. The study was performed over the western hemisphere during 18 months between January 2010 and June 2011. During this period, WWLLN showed 11% of coincidence during the entire region under study with higher values over oceanic regions than over continental regions.

Hutchins et al. (2012a) developed a model to calculate the relative detection efficiency of the WWLLN using the detected energy per stroke. This model allows to correct the global stroke density detected by WWLLN as if this network had a uniform spatial and temporal coverage. Hutchins et al. (2012a) applied the model to the lightning data detected by WWLLN from April 2009 through October 2011. They found an increase in the global average relative detection efficiency over the years which is highly correlated with the total number of operational stations of the network. Therefore, the lightning activity of different and distant regions can be compared since the model compensates for the uneven global coverage of the network and for the variations in propagation of the very low frequency signal. However, the model does not provide an absolute detection efficiency and only allows to perform comparative studies on lightning activity.

These studies of the WWLLN capability have shown a continuous improvement of this network. This improvement is due to the addition of new stations and to the upgrade of the detection algorithm. Therefore, periodic studies are necessary to assess the current WWLLN detection efficiency. Thereupon, the aim of this study is to evaluate the lightning data detected by WWLLN between the years 2012 and 2014 using the lightning data provided by LIS. This analysis would give a new insight on WWLLN and LIS detection capabilities, which would improve to quality of the lightning data provided by both systems. Finally, based on the analysis performed, a

correction method for WWLLN data is developed. This correction method would allow a broad use of the lightning data provided by WWLLN, expanding the capability of this network.

Methodology

The data used in this study came from the Lightning Imaging Sensor (LIS), on board the Tropical Rainfall Measuring Mission satellite, and from the World Wide Lightning Location Network.

The LIS instrument is a sensor designed to detect the total lightning activity, intra-cloud and cloud-to-ground lightning, of any storm that passes through the field of view of its sensor. The LIS instrument detects the optical pulses associated with changes in cloud brightness at each pixels. Pixels on LIS sensors exceeding the background threshold are defined as an event. Spatially adjacent events during the same observation window are clustered into groups. If a set of groups are sequentially separated in time by no more than 330 ms and in space by no more than 5.5 km, this set is grouped into a flash. Finally, the flashes that are separated in space by no more than 16.5 km are grouped into areas (Christian et al, 2000; Mach et al., 2007). These different products (Events, Groups, Flashes and Areas) are provided by LIS and can be related to different lightning-storm characteristics.

The LIS instrument detects lightning between 38°N and 38°S latitude and it has a detection efficiency which depends on the local time. Boccippio et al. (2002) predict a flash detection efficiency of $93 \pm 4\%$ and $73 \pm 11\%$ at night and at noon, respectively; while Cecil et al., (2014) present the hourly detection efficiency for LIS which is within the range of 88% overnight to 69% near local noon.

The WWLLN is a ground-base network with world-wide and real-time detection. The WWLLN detects the very low frequency (VLF) wave packet emitted by lightning. The network uses the Time of Group Arrival (TOGA), along with minimization methods, to locate the lightning (Dowden et al., 2002; Rodger et al., 2009). The WWLLN preferentially detects cloud-to-ground lightning with the greatest peak current and detects, generally, a single stroke within a lightning flash (Abarca et al., 2010; Abreu et al., 2010). However, Rudlosky and Shea (2013) found an average multiplicity (number of WWLLN strokes per LIS flash) of 1.5 during the period between 2009 and 2012 over the western hemisphere. Recently, an upgrade of the WWLLN allows the network to measure the radiated VLF stroke energy which is related to the return-stroke peak current (Hutchins et al., 2012b) of the stroke detected by WWLLN.

In this study, flashes detected by LIS and strokes detected by WWLLN between the years 2012 and 2014 were analyzed. The flashes detected by LIS are multiple optical pulses that occur in the same storm cell within 330 ms and 5.5 km of each other (Mach et al., 2007). Therefore, reported for each flash are the initial time of the flash, the flash duration, the location (Latitude - Longitude) of the flash centroid, its size (Area) and the number of groups assigned to the flash. The location, time of occurrence and the radiated VLF energy is reported by WWLLN for each of the strokes detected.

Different studies have compared the strokes detected by WWLLN to flashes and groups detected by LIS (Rudlosky and Shea, 2013; Thompson et al., 2014) to evaluate the WWLLN detection efficiency. These studies have used different matching criteria to assign flashes or groups detected by LIS to the strokes detected by WWLLN in order to find the WWLLN detection efficiency relative to LIS. However, these studies did not filter WWLLN strokes for LIS view times as only WWLLN detection efficiency relative to LIS was evaluated. In this study only WWLLN strokes during the LIS view

times are used so that LIS detection efficiency relative to WWLLN can also be measured. During the three years under analysis, between 38°N and 38°S latitude, LIS detected more than 4×10^6 flashes while WWLLN detected more than 600×10^6 strokes. On the areas under LIS observation, WWLLN detected over 6×10^5 strokes.

A match between the strokes detected by WWLLN and the flashes detected by LIS was performed, using the strokes detected by WWLLN in the LIS field of view. A stroke detected by WWLLN was assigned to a LIS flash every time the WWLLN stroke met the following criteria:

- the WWLLN stroke had occurred 200 ms before, during or 200 ms after a LIS flash, and
- the location of the WWLLN stroke is within a distance less or equal to $(\text{Area}/\pi)^{0.5} + 20$ km of the LIS flash centroid.

The time and distance thresholds (200 ms and 20 km) were selected based on the results of different tests using different threshold values. Figure 1 shows the ratio between the matched strokes and to the total strokes detected by WWLLN in the LIS field of view using different time and distance thresholds. As can be observed on Figure 1, the values of 200 ms and 20 km for time and distance correspond to values where an increment of these values results in a no longer significant increment on the number of the matched strokes. On the other hand, a more restrictive criteria strongly diminished the number of the matched strokes. Therefore, these broad criteria were selected to ensure the identification of all possible matches.

Results and discussion

Figure 2 shows the spatial distribution, using a spatial resolution of $2^\circ \times 2^\circ$, of the flashes detected by LIS (Upper panel), the distribution of the strokes detected by

WWLLN in the areas under LIS observation (Middle panel) and the relative detection efficiency (Lower panel) between 2012 and 2014. The relative detection efficiency was computed as the ratio between the strokes detected by WWLLN, in the areas under LIS observation, and the flashes detected by LIS.

Both detection systems present a similar global pattern of flash and stroke distributions with lightning detected preferably over land. A Pearson correlation coefficient of 0.62 ($p < 10^{-4}$) was computed between both lightning datasets. The high lightning activity centers over Africa, South America and Maritime Continent, which have been long known (Whipple, 1929), could be observed on both maps. However, WWLLN shows a better ability to detect strokes over Central and North America with respect to other regions of the globe. This relative better performance of WWLLN is in agreement with the finding of Rudlosky and Shea (2013) and Thompson et al. (2014). Meanwhile, WWLLN presents a lower detection capability relative to LIS over South America, Africa and over India (Tibetan plateau).

As reported by Rudlosky and Shea (2013) and Thompson et al., (2014), over oceanic regions, there are areas with more strokes detected by WWLLN than flashes detected by LIS. This better ability of WWLLN respect to LIS, over oceanic regions, seems to be the results of a better detection capability of WWLLN over the oceans. Further, the different optical scattering properties of the storms over land and ocean (Peterson and Liu, 2011) together with the different properties of lightning flashes that occur over continental and oceanic regions also seem to improve the ability of WWLLN respect to LIS.

Boccippio et al. (2000) reported that the flashes detected by OTD and by LIS are brighter and larger over the ocean than the flashes detected over continental regions. However, they were unable to asses if these differences are due to difference on the

flashes features or due to difference in the optical scattering properties of the storms. Different studies (Peterson and Liu, 2013; Bitzer et al., 2016; Peterson et al., 2017) had shown that the flashes detected by LIS over oceanic regions are larger, with a longer duration and brighter than the flashes detected over continental regions. Also, Peterson et al. (2016) reported that flashes over the ocean contain more groups and are more prone to propagate horizontally than flashes over land.

On the other hand, WWLLN is capable of detecting strokes with lower energy over the ocean respect to land given that the VLF signal is less attenuated over the oceans than over land during signal propagation. Therefore, WWLLN has a bias to detect the highest energy strokes over land and more lower energy strokes over oceanic regions (Hutchins et al., 2012b). Furthermore, there is evidence that lightning over the oceans have higher energy than lightning over land (Said et al., 2013; Hutchins et al., 2013) and WWLLN detects preferentially the more energetic lightning (Abarca et al., 2010; Abreu et al., 2010).

The local time distribution of the flashes detected by LIS and the strokes detected by WWLLN, in the field of view of LIS, are shown on Figure 3 (Upper panel). The datasets are strongly correlated with a Pearson correlation coefficient of 0.96 ($p < 10^{-4}$), which indicates that WWLLN is able to detect the diurnal cycle on the lightning activity. However, the amplitude of the diurnal lightning cycle detected by WWLLN was much lower than the amplitude detected by LIS. While LIS reports seven times more flashes during local afternoon than during early morning, WWLLN only reports two times more strokes. This difference seems to be due to the low detection efficiency of the network over Africa and over South America, which have been reported as the main contributors to the peak on the lightning diurnal cycle (Blakeslee et al., 2014). These differences on the detected amplitude of the diurnal lightning cycle is reflected on

the local time distribution of the relative detection efficiency (Figure 3, Lower panel). The relative detection efficiency increase in early local morning and reach a maximum values at around 9:00 (local time). After that, the relative detection efficiency decrease to a minimum value during local afternoon, which correspond to the diurnal cycle maximum.

The good agreement between the spatial and time distributions of both lightning datasets shows that, despite the lower detection efficiency of the WWLLN, this network is able to detect the main features of the global lightning activity.

With the matching criteria adopted, 434553 WWLLN strokes were assigned to 288047 LIS flashes. The amount of strokes matched is around 66% of the total strokes detected by WWLLN in the LIS field of view. The number of strokes matched to the flashes indicates that WWLLN is capable of detecting more than one stroke per flash. Defining the multiplicity as the ratio of the number of matched WWLLN strokes to the number of matched LIS flashes, WWLLN presents a global mean multiplicity of 1.5. Although, WWLLN is capable of detecting multiple strokes during a LIS flash, 70% of the matched flashes were coincident with a single stroke.

Figure 4 shows the spatial distribution of the multiplicity using a spatial resolution of $2^{\circ} \times 2^{\circ}$. The higher values of the multiplicity are found over oceanic regions and over Central America. These regions also show the higher relative detection efficiency of WWLLN relative to LIS (Figure 2 Lower panel) as reported by Rudlosky and Shea (2013) and Thompson et al., (2014). This better detection ability of WWLLN over the oceans seems to be due to the bias of this network to detect strokes with lower energy over oceanic regions (Hutchins et al., 2012b) and the strength of strokes over these regions. Further, as reported by Peterson et al. (2016), the flashes detected by LIS over

ocean contain more groups than the flashes over land, which implies that flashes over oceanic regions probably have higher multiplicity.

Figure 5 shows the difference between the time of occurrence of the matched strokes and the initiation time of the matched flashes (Upper panel) and the distance between the matched strokes and the flash centroid (Lower panel). Given that the flash duration and area of the flashes are used in the matching criteria, the time differences and distances of the matched strokes can be larger than the threshold value used as can be observed in Figure 5. The mean (median) time difference and distance are 114 ms (24 ms) and 10 km (9 km), respectively. As can be observed, almost 90% of the matched strokes show a positive time difference which implies that these matched strokes were detected after the initiation of the matched flash. Although the parameters calculated cannot be taken as the WWLLN accuracy since different aspects of a lightning are compared, these values can be used as an indicator of the WWLLN detection ability. The values obtained agree with the accuracy of the WWLLN reported by Rudlosky and Shea (2013).

The remaining WWLLN strokes (221732 strokes, ~34%) detected in the LIS field of view were not assigned to any LIS flash (unmatched strokes). As mentioned before, different time and distance thresholds were examined. Using values larger than 200 ms and 20 km (up to 500 ms and 50 km) only improved the number of matched strokes up to 5% of the total strokes (see Figure 1). With a more restrictive matching criteria (0 ms and 0 km), the number of matched strokes decreased to around 40% of the total strokes detected in the LIS field of view. Given that previous studies do not show evidence that WWLLN detects false positives (Lay et al., 2004; Rodger et al., 2005; Rodger et al., 2006; Jacobson et al., 2006; Abarca et al., 2010; Abreu et al., 2010), these unmatched

strokes indicate that WWLLN is capable of detecting strokes that are not detected by LIS.

Figure 6 shows the spatial distribution, with a spatial resolution of $2^{\circ} \times 2^{\circ}$, of the matched strokes (Upper panel), unmatched strokes (Middle panel) and the ratio of unmatched to matched strokes (Lower panel). A similar pattern of the spatial distribution of the matched and unmatched strokes can be observed with a Pearson correlation coefficient of 0.95 ($p < 10^{-4}$). The spatial distribution of the ratio between the unmatched and matched strokes (Figure 6 Lower panel) does not show a clear geographical dependence on the location of the unmatched strokes.

Figure 7 (Upper panel) shows the local time distribution of the matched (Dashed line) and unmatched strokes (Solid line). The local time distribution of the LIS detection efficiency, adapted by the values reported by Cecil et al. (2014, Table 2), is also showed on Figure 7 (Upper panel) (Dotted line). The time distribution between the matched and unmatched strokes shows a high correlation with a Pearson correlation coefficient of 0.92 ($p < 10^{-4}$). An analysis of the energy reported by WWLLN, using the regression method proposed by Hutchins et al. (2013), does not show a significant difference between the energy distribution of the matched and unmatched strokes.

On Figure 7 (Lower panel) is shown the hourly variation of the ratio between the matched strokes and the total strokes detected by WWLLN in the areas under LIS observation (solid line) and the LIS detection efficiency (Cecil et al., 2014) (dotted line). As can be observed, the ratio between the matched strokes and the total strokes shows a good agreement with the hourly distribution of LIS detection efficiency with both distribution showing minimum values at local noon. However, the ratio between the matched strokes and the total strokes shows several oscillations which seems to be due to the temporal resolution used on the calculations. Despite this oscillations, the

hourly variations on LIS detection efficiency seems to explain less than 10% of the unmatched strokes. Therefore, the detection efficiency of LIS cannot fully explain the unmatched strokes found in this study. Thomas et al. (2000) compared the observation from the Lightning Mapping Array (LMA) with LIS data. These researchers found an excellent correlation between both data sets. However, they reported that LIS presents different detection efficiencies for intracloud (IC) and cloud-to-ground (CG) discharges. While almost all IC discharges detected by LMA were detected by LIS, only 60% of CG discharges were detected by LIS. The CG discharges not detected by LIS correspond to CG discharges confined below an altitude of 7 km. Given that LIS is an optical sensor that detects luminous events, the amount of light, from a discharge, that can reach the sensor will depend on the optical depth between the discharge and the cloud surface. Therefore, optical sensors present different detection efficiencies for IC and CG, as was reported by Thomas et al. (2000), with a bias to detect IC discharges. On the other hand, WWLLN is most sensitive to CG discharges than to IC discharges (Abarca et al. 2010). This bias of the network is due to the fact that WWLLN detects the VLF radio wave emitted by lightning and that CG discharges radiate stronger in VLF than IC discharges. Therefore, the unmatched strokes seem to be due to the different detection bias reported for both detection systems. However, further analysis is needed to identify different case studies which could provide an insight on these unmatched strokes.

Correction to WWLLN lightning data

The analysis performed and previous studies had shown that WWLLN had a low detection efficiency, which also shows spatial and temporal variations. This low detection ability, and its variations, do not allow for the use of the lightning data

provided by WWLLN on more accurate studies of the global lightning activity and to perform comparative studies of the lightning climatology between different regions. Several studies had tried to find the detection efficiency of the network using the lightning data provided by different ground-base network and satellite systems (Lay et al., 2004; Jacobson et al., 2006; Rodger et al., 2009; Abarca et al., 2010; Abreu et al., 2010; Rudlosky and Shea, 2013; Thompson et al., 2014). However, these studies are spatially and temporally limited due to the lack of available lightning data. Hutchins et al. (2012a) presented a model based on the stroke energy detected by WWLLN that allows computation of the global stroke distribution as if the WWLLN shows a uniform global detection efficiency. Nevertheless, this model does not provide an overall absolute detection efficiency for the network. Therefore, the development of an algorithm which allows computation of the detection efficiency of WWLLN will expand the capability of the network and facilitate a broad use of the lightning data provided by WWLLN. Thus, a correction method of the WWLLN lightning data is proposed based on the data provided by LIS.

Let F be the number of flashes that actually occurred in the LIS field of view. Then, the probability that LIS detects a flash can be defined as the ratio between the flashes detected by this instrument (F_{LIS}) and F ,

$$P_{LIS} = F_{LIS} F^{-1} \quad (1)$$

In the same way, the probability that WWLLN and LIS detect the same flash can be defined as the ratio between the matched flashes (F_M) and F ,

$$P_{W,LIS} = F_M F^{-1} \quad (2)$$

Given that WWLLN and LIS are independent detection systems, the probability $P_{W,LIS}$ can also be defined as,

$$P_{W,LIS} = P_{LIS} P_W \quad (3)$$

Where P_W is the probability that WWLLN will detect a flash. From these equations, it is possible to derive an expression for P_W as follows,

$$P_W = F_M F_{LIS}^{-1} \quad (4)$$

The expression obtained for P_W is independent of the real number of flashes (F). Therefore, in order to calculate the detection probability of WWLLN, it is not necessary to correct LIS data by its detection efficiency. However, these equations are valid if both detection systems, LIS and WWLLN, do not present false positives.

Figure 8 shows the P_W distribution computed using Eq. 4 for a $2^\circ \times 2^\circ$ spatial resolution. P_W values range between 0.01 and 0.1 (1% and 10%) for continental regions while over oceanic regions P_W shows values higher than 0.2 (20%). The map shows a good agreement with the analysis performed by Rudlosky and Shea (2013) and Thompson et al. (2014) for the western hemisphere, with higher probability over Central and North America and over oceanic regions.

To correct the lightning data provided by WWLLN, given that the values of P_W were derived using flashes, it is necessary to cluster the strokes detected by this network into flashes. Different methods have been proposed to cluster the strokes into flashes using the times of occurrence and locations criteria. An alternative approach to determine the

number of WWLLN flashes is using the multiplicity computed in the previous analysis (Figure 4). Therefore, the number of strokes detected by WWLLN on each grid box was divided by the value of multiplicity of the corresponding grid box to group the strokes into flashes. This approach differs from traditional stroke to flash algorithms but is expected to provide a good estimation of the number of flashes detected by WWLLN.

These estimated flashes were corrected using the values of P_w found. Figure 9 shows the corrected flash density based on the strokes detected by WWLLN between 2012 and 2014. The correction applied enhances the lightning activity over the areas where the WWLLN showed lower detection capability (South America, Africa and over India). The corrected flash density and the flash density computed with the lightning data provided by LIS show a high correlation with a Pearson correlation coefficient of 0.96 ($p < 10^{-4}$).

WWLLN detected around 6 strokes s^{-1} , which represent a lightning flash rate of 4 flashes s^{-1} using a mean global multiplicity of 1.5. The mean value of P_w found in this study is 0.07 and therefore, the lightning flash rate detected by WWLLN is 60 fl s^{-1} . This value is in agreement with the values determined by satellite measurements (Cecil et al., 2014; Christian et al., 2003).

The corrected lightning activity shows good agreement with the lightning activity reported by other detection systems, which give confidence on the proposed method. However, the multiplicity and the values of P_w used on the correction depend on the matching criteria used to compute the matched flashes between both datasets. The use of a more restrictive criteria strongly diminished the number of the matched strokes and therefore, decreased the detection probability values. Further analysis is needed to study the robustness of the correction method proposed.

Summary

The flashes detected by LIS were compared to the strokes detected by WWLLN in the LIS field of view between the years 2012 and 2014. During these three years, LIS detected more than 40×10^5 flashes on the tropical region while WWLLN detected around 6×10^5 strokes in the field of view of LIS.

The events detected by both systems show a similar spatial distribution with a high time correlation showing that WWLLN performance is good enough to detect the main features of tropical lightning despite of the low detection efficiency reported for this network.

Using a matching criteria, almost 70% of the strokes detected by WWLLN in the LIS field of view were matched with flashes detected by LIS with a mean (median) time difference and distance of 114 ms (24 ms) and 10 km (9 km), respectively. Although most of the flashes were matched with single strokes, several matched LIS flashes had multiple coincident WWLLN strokes, which means that WWLLN is capable of detecting more than one stroke per flash with a mean multiplicity of 1.5.

Around 30% of strokes detected by WWLLN in the LIS field of view were not assigned to any flash detected by LIS. These unmatched strokes show a spatial, time and energy distribution similar to that of the matched strokes. These unmatched strokes seem to correspond to cloud-to-ground lightning given that LIS shows a lower detection efficiency for this type of discharge while WWLLN preferentially detects these kind of events. Although, satellite detection systems, as LIS and GLM, present high detection efficiencies, the results of this study show that optical detection systems can miss a significant amount of lightning events, particularly cloud-to-ground flashes on the lower part of the storms. Therefore, in order to obtain high quality lightning data, the different detection systems, satellite and ground-base, should be used together.

A correction on the lightning activity detected by WWLLN is proposed which allows for a more extensive use of the lightning data provided by the network. Using the correction, WWLLN presents a lightning flash rate of 60 fl s^{-1} , which is in agreement with reported values.

Acknowledgments

The author wishes to thank the World Wide Lightning Location Network (<http://wwlln.net>), collaboration among over 50 universities and institutions, for providing the lightning location data used in this paper. He is grateful to the NASA Global Hydrology Resource Center DAAC for LIS data.

This work was supported by SECYT-UNC, CONICET and FONCYT.

The authors want to thank to the anonymous reviewers for their useful comments and suggestions that greatly improved the quality of this paper.

References

Abarca, SF, Corbosiero, KL, Galarneau, TJ. 2010. An evaluation of the worldwide lightning location network (WWLLN) using the national lightning detection network (NLDN) as ground truth. *Journal of Geophysical Research: Atmospheres*, 115(D18).

Abreu, D, Chandan, D, Holzworth, RH, Strong, K. 2010. A performance assessment of the World Wide Lightning Location Network (WWLLN) via comparison with the Canadian Lightning Detection Network (CLDN). *Atmospheric Measurement Techniques*, 3(4), 1143-1153.

Betz, HD, Schmidt, K, Laroche, P, Blanchet, P, Oettinger, WP, Defer, Dziewit, EZ, Konarski, J. 2009. LINET—an international lightning detection network in Europe. *Atmospheric Research*, 91(2), 564-573.

Bitzer, PM, Burchfield, JC, Christian, HJ. 2016. A Bayesian approach to assess the performance of lightning detection systems. *Journal of Atmospheric and Oceanic Technology*, 33(3), 563-578.

Blakeslee, RJ, Mach, DM, Bateman, MG, Bailey, JC. 2014. Seasonal variations in the lightning diurnal cycle and implications for the global electric circuit. *Atmospheric Research*, 135, pp. 228-243.

Boccippio, DJ, Goodman, SJ, Heckman, S. 2000. Regional differences in tropical lightning distributions, *J. Appl. Meteorol.*, 39, 2231–2248.

Boccippio, DJ, Koshak, WJ, Blakeslee, RJ. 2002. Performance assessment of the Optical Transient Detector (OTD) and Lightning Imaging Sensor. Part I: Predicted diurnal variability, *J. Atmos. Oceanic Technol.*, 19, 1318-1332.

Cecil, DJ, Buechler, DE, Blakeslee, RJ. 2014. Gridded lightning climatology from TRMM-LIS and OTD: Dataset description. *Atmospheric Research*, 135, 404-414.

Christian, HJ, Blakeslee, RJ, Goodman, SJ. 1992. Lightning imaging sensor (LIS) for the earth observing system.

Christian, HJ, Blakeslee, RJ, Goodman, SJ, Mach, DM, 2000. The Algorithm Theoretical Basis Document (ATBD) for the Lightning Imaging Sensor (LIS). Available from http://eosps0.gsfc.nasa.gov/eos_homepage/for_scientists/atbd/docs/LIS/atbd-lis-01.pdf.

Christian, HJ, Blakeslee, RJ, Boccippio, DJ, Boeck, WL, Buechler, DE, Driscoll, KT, ... Stewart, MF. 2003. Global frequency and distribution of lightning as observed from space by the Optical Transient Detector. *Journal of Geophysical Research: Atmospheres*, 108(D1).

Cummins, KL, Mur, MJ. 2009. An overview of lightning locating systems: History, techniques, and data uses, with an in-depth look at the US NLDN. *Electromagnetic Compatibility, IEEE Transactions on*, 51(3), 499-518.

DeMaria, M, DeMaria, RT, Knaff, JA, Molenaar, D. 2012. Tropical cyclone lightning and rapid intensity change. *Mon. Weather Rev.* 140, 1828–1842.

Dockendorff, D, Spring, K. 2005. The Canadian Lightning Detection Network-Novel approaches for performance measurement and network management. In Proceedings, *WMO Technical Conference on Instruments and Methods of Observation (TECO)*, Bucharest, Romania.

Dowden, RL, Brundell, JB, Rodger, CJ. 2002. VLF lightning location by time of group arrival (TOGA) at multiple sites. *Journal of Atmospheric and Solar-Terrestrial Physics*, 64(7), 817-830.

Garreaud, RD, Nicora, MG, Bürgesser, RE, Avila, EE. 2014. Lightning in Western Patagonia, *J. Geophys. Res. Atmos.*, 119, doi:10.1002/2013JD021160.

Goodman, SJ, Blakeslee, RJ, Koshak, WJ, Mach, D, Bailey, J, Buechler, D, Carey, L, Schultz, C, Bateman, M, McCaul Jr., E, Stano, G. 2013. The GOES-R geostationary lightning mapper (GLM). *Atmospheric Research*, 125, 34-49.

Heckman, S. 2014. ENTLN Status Update. XV International Conference on Atmospheric Electricity, 15-20 June 2014, Norman, Oklahoma, U.S.A.

Hutchins, ML, Holzworth, RH, Brundell, JB, Rodger, CJ. 2012a. Relative detection efficiency of the world wide lightning location network. *Radio Science*, 47(6).

Hutchins, ML, Holzworth, RH, Rodger, CJ, Brundell, JB. 2012b. Far-field power of lightning strokes as measured by the World Wide Lightning Location Network. *Journal of Atmospheric and Oceanic Technology*, 29(8), 1102-1110.

Hutchins, ML, Holzworth, RH, Virts, KS, Wallace, JM, Heckman, S. 2013. Radiated VLF energy differences of land and oceanic lightning. *Geophysical Research Letters*, 40(10), 2390-2394.

Jacobson, AR, Holzworth, R, Harlin, J, Dowden, R, Lay, E. 2006. Performance assessment of the World Wide Lightning Location Network (WWLLN), using the Los Alamos Sferic Array (LASA) as ground truth, *J. Atmos. Ocean. Tech.*, 23, 1082–1092.

Lay, EH, Holzworth, RH, Rodger, CJ, Thomas, JN, Pinto Jr., O, Dowden, R. 2004. WWLL global lightning detection system: Regional validation study in Brazil, *Geophys. Res. Lett.*, 31, L03102, doi:10.1029/2003GL018882.

Mach, DM, Christian, HJ, Blakeslee, RJ, Boccippio, DJ, Goodman, SJ, Boeck, WL. 2007. Performance assessment of the optical transient detector and lightning imaging sensor. *Journal of Geophysical Research: Atmospheres*, 112(D9).

Mecikalski, JR, Li, X, Carey, LD, McCaul, EW, Coleman, TA. 2013. Regional comparison of GOES cloud-top properties and radar characteristics in advance of first-flash lightning initiation. *Mon. Wea. Rev.* 141, 55–74.

Peterson, M, Liu, C. 2011. Global statistics of lightning in anvil and stratiform regions over the tropics and subtropics observed by the Tropical Rainfall Measuring Mission. *Journal of Geophysical Research: Atmospheres*, 116(D23).

Peterson, M, Liu, C. 2013. Characteristics of lightning flashes with exceptional illuminated areas, durations, and optical powers and surrounding storm properties in the tropics and inner subtropics. *Journal of Geophysical Research: Atmospheres*, 118(20).

Peterson, M, Deierling, W, Liu, C, Mach, D, Kalb, C. 2017. The properties of optical lightning flashes and the clouds they illuminate, *J. Geophys. Res. Atmos.*, 122, 423–442, doi:10.1002/2016JD025312.

Reeve, N, Toumi, R. 1999. Lightning activity as an indicator of climate change. *Q.J.R. Meteorol. Soc.*, 125: 893–903.

Rodger, CJ, Brundell, JB, Dowden, RL. 2005. Location accuracy of VLF World-Wide Lightning Location (WWLL) network: Post-algorithm upgrade, *Ann. Geophys.*, 23, 277–290, doi:10.5194/angeo-23-277-2005.

Rodger, CJ, Werner, S, Brundell, JB, Lay, EH, Thomson, NR, Holzworth, RH, Dowden, RL. 2006. Detection efficiency of the VLF World-Wide Lightning Location Network (WWLLN): initial case study, *Ann. Geophys.*, 24, 3197–3214, doi:10.5194/angeo-24-3197-2006.

Rodger, CJ, Brundell, JB, Holzworth, RH, Lay, EH, Crosby, NB, Huang, TY, Rycroft, MJ. 2009, April. Growing detection efficiency of the world wide lightning location network. *In AIP Conf. Proc.*, Vol. 1118, No. 118, pp. 15-20.

Romps, DM, Seeley, JT, Vollaro, D, Molinari, J. 2014. Projected increase in lightning strikes in the United States due to global warming. *Science*, 346(6211), 851-854.

Rudlosky, SD, Shea, DT. 2013. Evaluating WWLLN performance relative to TRMM/LIS. *Geophysical Research Letters*, 40(10), 2344-2348.

Said, RK, Cohen, MB, Inan, US. 2013. Highly intense lightning over the oceans: Estimated peak currents from global GLD360 observations. *Journal of Geophysical Research: Atmospheres*, 118(13), 6905-6915.

Schultz, CJ, Petersen, WA, Carey, LD. 2011. Lightning and severe weather: a comparison between total and cloud-to-ground lightning trends. *Weather Forecast.* 26, 744–755.

Shevtsov, BM, Firstov, PP, Cherneva, NV, Holzworth, RH, Akbashev, RR. 2015. Lightning and electrical activity during the Shiveluch volcano eruption on 16 November 2014, *Nat. Hazards Earth Syst. Sci. Discuss.*, 3, 6745–6755.

Soula, S, Kigotsi Kasereka, J, Georgis, JF, Barthe, C. 2016. Lightning climatology in the Congo Basin, *Atmospheric Research* 178–179, pp. 304–31.

Thomas, RJ, Krehbiel, PR, Rison, W, Hamlin, T, Boccippio, DJ, Goodman, SJ, Christian, HJ. 2000. Comparison of ground-based 3-dimensional lightning mapping observations with satellite-based LIS observations in Oklahoma. *Geophysical research letters*, 27(12), pp. 1703-1706.

Thompson, KB, Bateman, MG, Carey, LD. 2014. A comparison of two ground-based lightning detection networks against the satellite-based Lightning Imaging Sensor (LIS). *Journal of Atmospheric and Oceanic Technology*, 31(10), 2191-2205.

Vaisala Global Lightning Dataset — Technology, Operations and Application Overview (2009) (9 p.

<http://www.vaisala.com/en/products/thunderstormandlightningdetectionsystems/Pages/GLD360.aspx>)

Virts, KS, Wallace, JM, Hutchins, ML, Holzworth, RH. 2015. Diurnal and seasonal lightning variability over the Gulf Stream and the Gulf of Mexico, *Journal of the Atmospheric Sciences* doi: <http://dx.doi.org/10.1175/JAS-D-14-0233.1>.

Whipple, FJW. 1929. On the association of the diurnal variation of electric potential gradient in fine weather with the distribution of thunderstorms over the globe. *Quarterly Journal of the Royal Meteorological Society*, 55(229), 1-18.

Xu, W, Adler, RF, Wang, NY. 2013. Improving geostationary satellite rainfall estimates using lightning observations: underlying lightning–rainfall–cloud relationships. *J. Appl. Meteor. Climatol.* 52, 213–229.

Captions

Figure 1: Ratio between the matched strokes and total strokes detected by WWLLN in the field of view of LIS for a constant distance threshold and with different time thresholds (Upper panel) and for a constant time threshold and with different distance thresholds (Lower Panel). Black circles represent a distance (time) threshold of 0 km (0 ms), open circles a distance (time) threshold of 5 km (50 ms), black triangle a distance (time) threshold of 10 km (100 ms), open triangle a distance (time) threshold of 20 km (200 ms), black square a distance (time) threshold of 30 km (300 ms), open square a distance (time) threshold of 40 km (400 ms) and black diamond a distance (time) threshold of 50 km (500 ms) in the Upper panel (Lower panel). The vertical black line

runs through the selected time (Upper panel) and distance (Lower Panel) thresholds.

The symbol \times marks the selected thresholds.

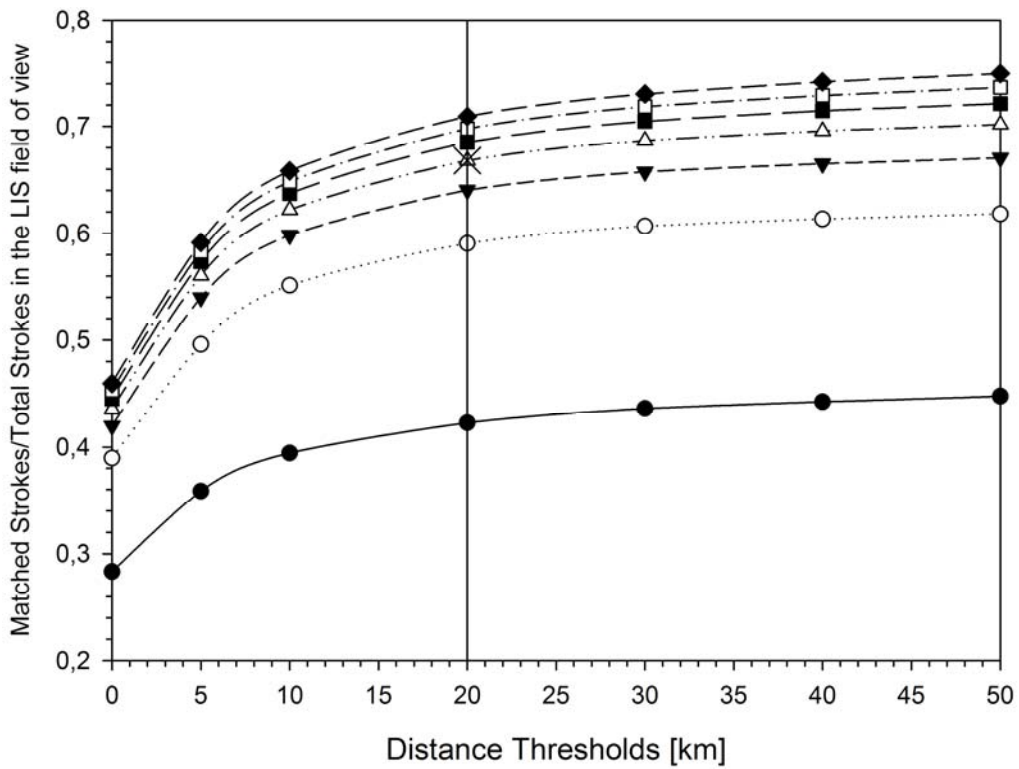
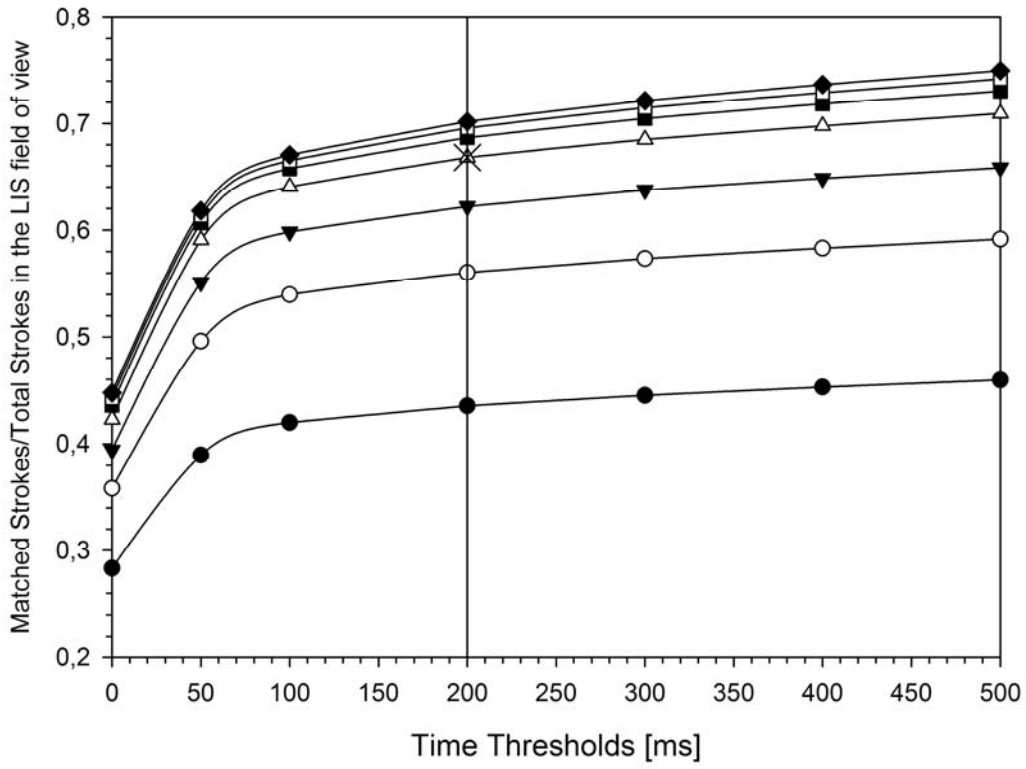


Figure 2: Spatial distribution of the flashes detected by LIS (Upper panel), the strokes detected by WWLLN in the LIS field of view (Middle panel) and WWLLN detection efficiency relative to the LIS (Lower panel) using a $2^\circ \times 2^\circ$ spatial resolution. Note the different color scales on the upper panels.

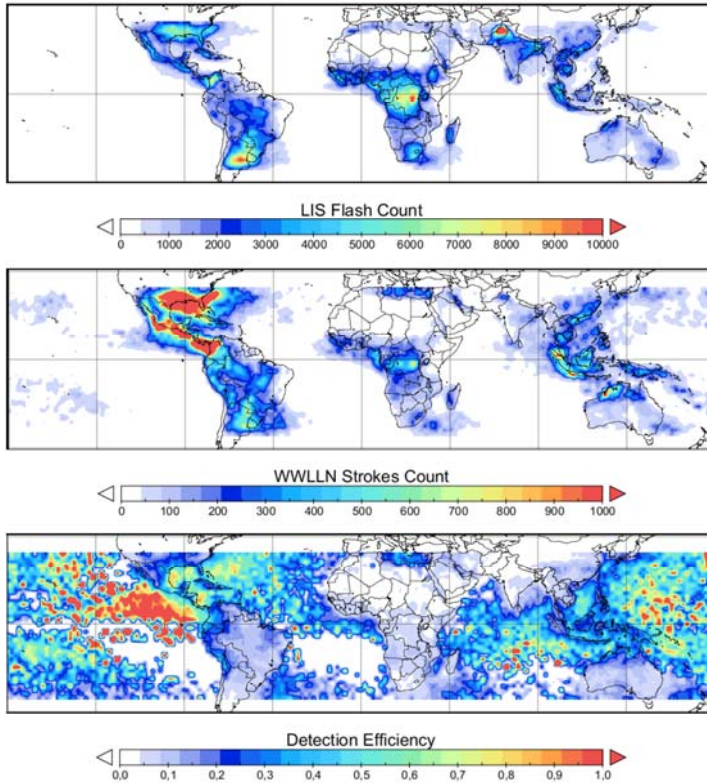


Figure 3: Local time distribution of the flashes detected by LIS (Solid line) and the strokes detected by WWLLN in the field of view of LIS (Dashed line) (Upper panel), and local time distribution of WWLLN detection efficiency relative to the LIS (Lower panel).

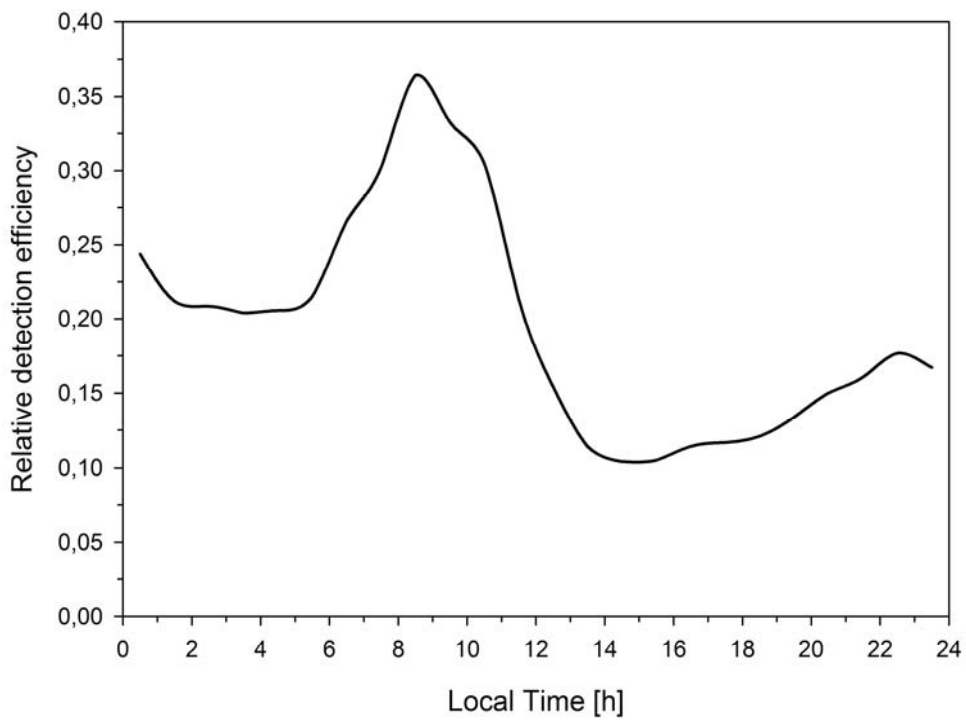
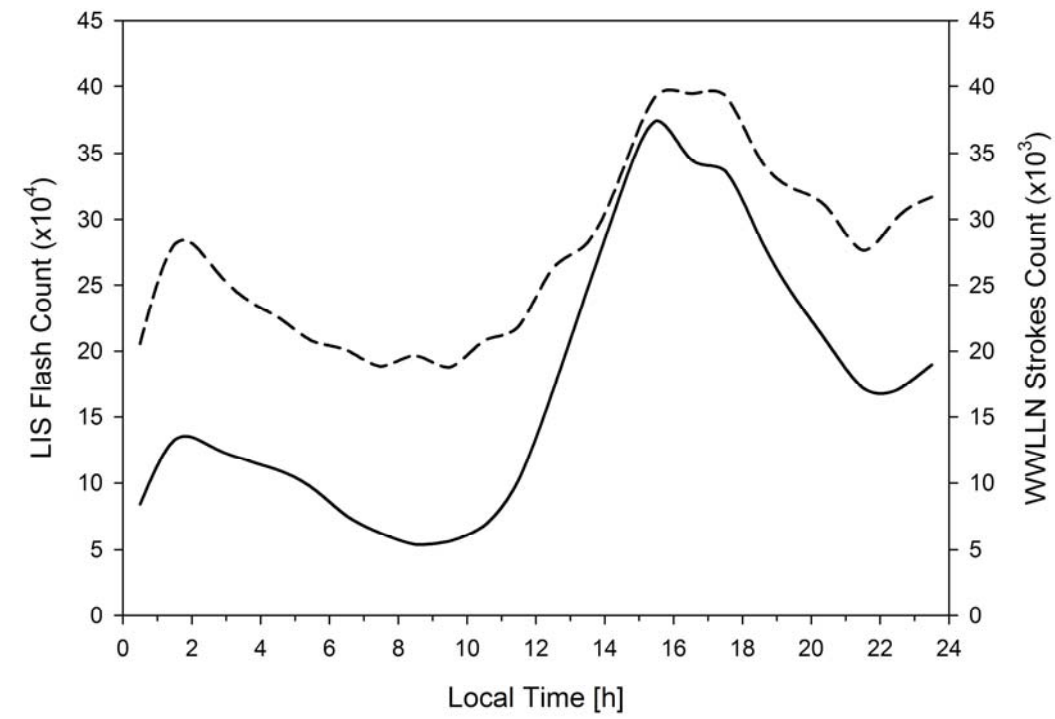


Figure 4: Spatial distribution of the computed multiplicity using a $2^\circ \times 2^\circ$ spatial resolution.

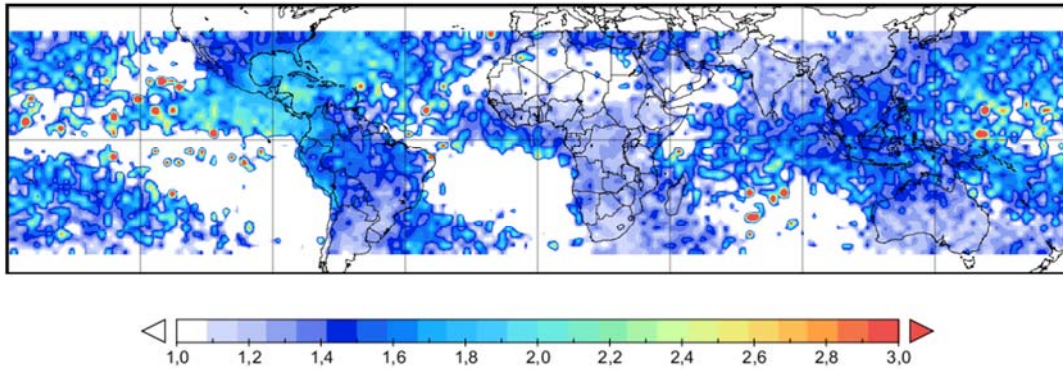


Figure 5: Difference between the time of occurrence of the matched strokes and time initiation of flashes (Upper panel). Data are grouped into a 10 ms bin size. Distance between the matched strokes and the flash centroid (Lower panel). Data are grouped into a 0.5 km bin size.

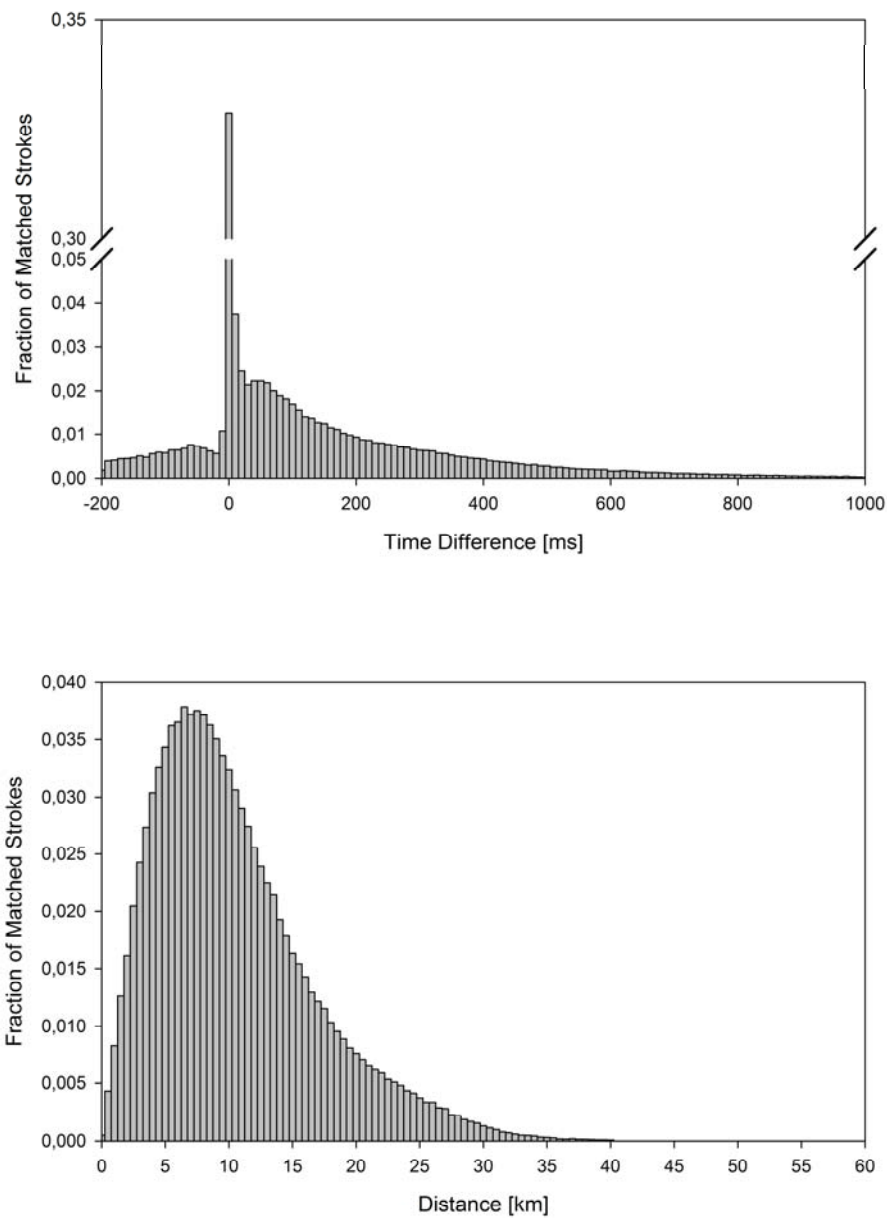


Figure 6: Spatial distribution of the matched strokes (Upper panel), the unmatched strokes (Middle panel) and the ratio of unmatched to matched strokes (Lower panel) using a $2^\circ \times 2^\circ$ spatial resolution.

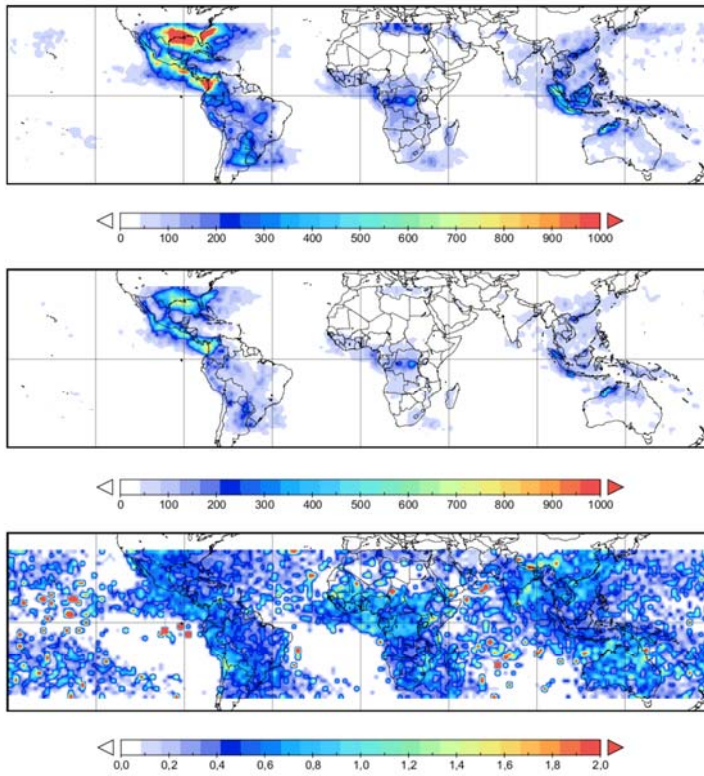


Figure 7: Local time distribution of the matched (Dashed line) and unmatched (Solid line) strokes, and the local time distribution of the detection efficiency of LIS (Dotted line) as reported by Cecil et. (2014) (Upper panel). Local time distribution of the ratio between the matched strokes and the total strokes (Solid line) and the local time distribution of the detection efficiency of LIS (Dotted line) as reported by Cecil et. (2014) (Lower panel).

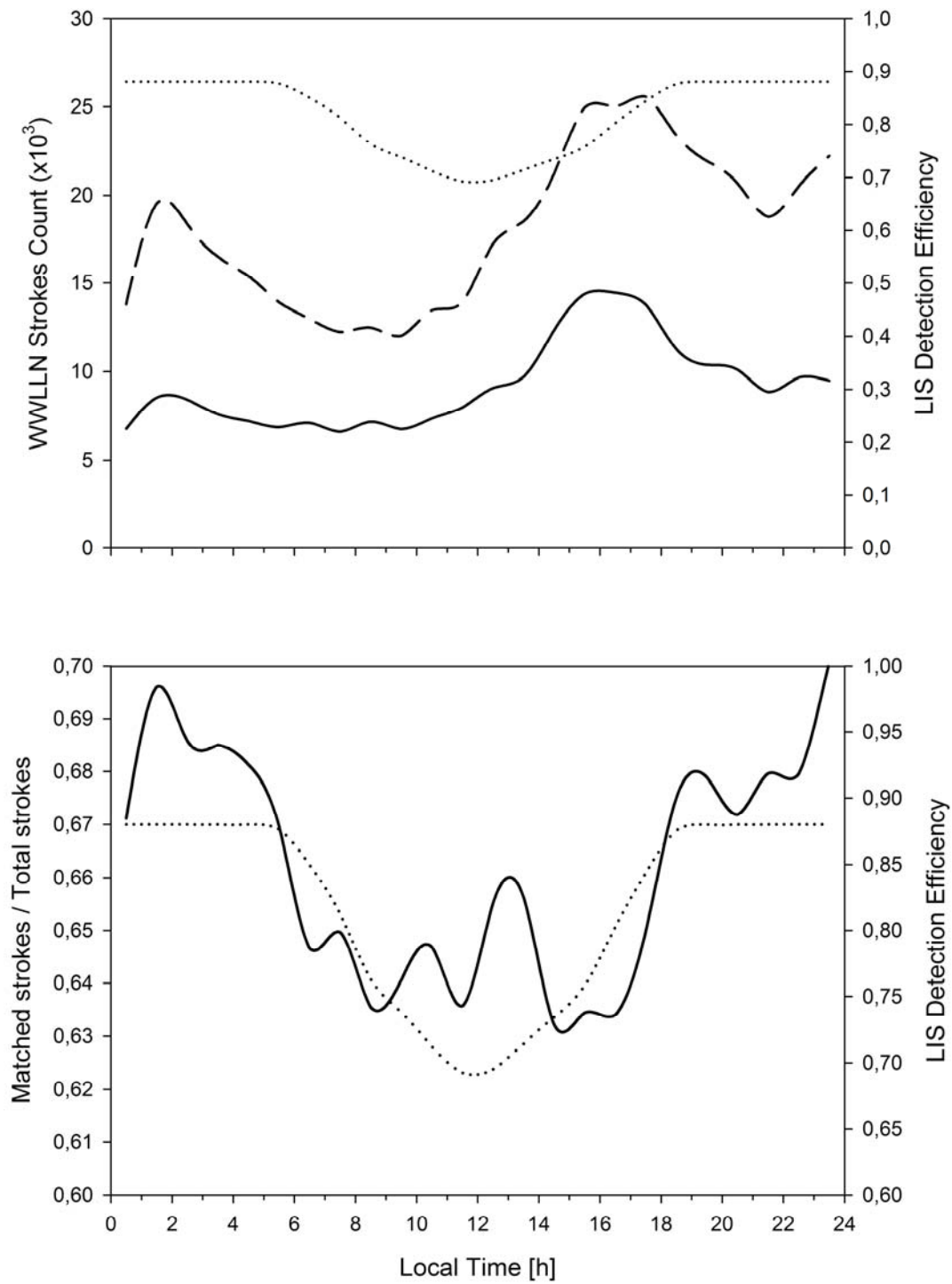


Figure 8: Spatial distribution of the WWLLN detection probability (P_w) using a $2^\circ \times 2^\circ$ spatial resolution.

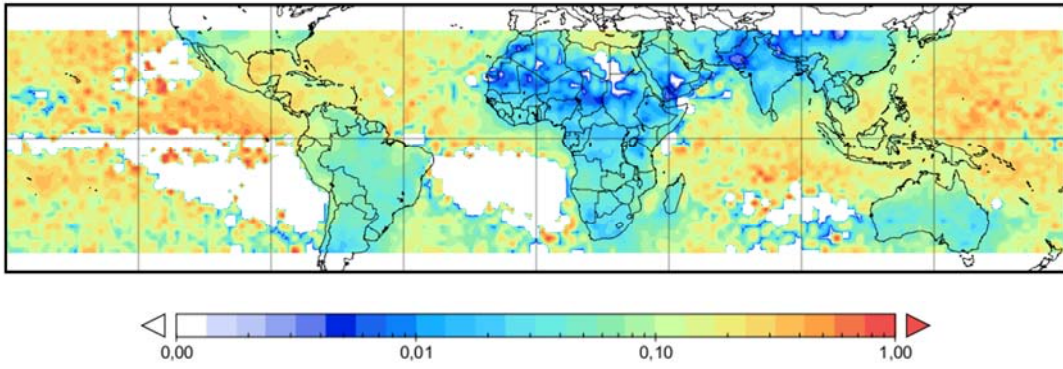


Figure 9: Flash density detected by WWLLN between 2012 and 2014 corrected by multiplicity and P_w using a $2^\circ \times 2^\circ$ spatial resolution.

